The Influence of Surface Chemistry on the Rate Capability of LiNi[subscript 0.5]Mn[subscript 0.5]O[subscript 2] for Lithium Rechargeable Batteries

Citation: Yabuuchi, Naoaki, Yi-Chun Lu, Azzam N. Mansour, Tadashi Kawaguchi, and Yang Shao-Horn. The Influence of Surface Chemistry on the Rate Capability of LiNi[subscript 0.5]Mn[subscript 0.5]O[subscript 2] for Lithium Rechargeable Batteries. Electrochemical and Solid-State Letters 13, no. 11 (2010): A158.© 2010 ECS - The Electrochemical Society.

Published Version: http://dx.doi.org/10.1149/1.3479664

Publisher: Electrochemical Society

Permanent Link: http://hdl.handle.net/1721.1/79591

Version: Final published version: final published article, as it appeared in a journal, conference proceedings, or other formally published context

Electrochemical and Solid-State Letters, **13** (11) A158-A161 (2010)
1099-0062/2010/13(11)/A158/4/$28.00 © The Electrochemical Society

The Influence of Surface Chemistry on the Rate Capability of $LiNi_{0.5}Mn_{0.5}O_2$ for Lithium Rechargeable Batteries

Naoaki Yabuuchi,[a,*] Yi-Chun Lu,[b] Azzam N. Mansour,[c,*] Tadashi Kawaguchi,[a] and Yang Shao-Horn[a,b,*,z]

[a]*Department of Mechanical Engineering and* [b]*Department of Material Science and Engineering, Massachusetts Institute of Technology, Cambridge, Massachusetts 02139, USA*
[c]*Naval Surface Warfare Center, Carderock Division, West Bethesda, Maryland 20817-5700, USA*

Subsequent annealing at 700°C enhances the rate capability of $LiNi_{0.5}Mn_{0.5}O_2$, delivering 180 mAh/g at 55°C and 8C rate compared to 50 mAh/g of $LiNi_{0.5}Mn_{0.5}O_2$ quenched from 1000°C. Although Rietvled refinement analyses of X-ray diffraction (XRD) data showed that there were no significant changes in the lattice parameters and cation distributions of the layered structure before and after annealing, XRD and X-ray photoelectron spectroscopy revealed that annealing significantly reduced surface impurity phases such as lithium carbonate and Mn^{3+}-containing species. The influence of surface chemistry changes on the rate capability of $LiNi_{0.5}Mn_{0.5}O_2$ was discussed.
 [DOI: 10.1149/1.3479664]

Manuscript submitted June 2, 2010; revised manuscript received July 19, 2010. Published August 17, 2010.

$LiNi_{0.5}Mn_{0.5}O_2$ is one of the promising positive electrode materials for large-scale lithium-ion batteries because of its high specific capacity (up to ~200 mAh/g),[1,2] thermal stability associated with redox-active Ni^{2+} and inactive Mn^{4+},[3,4] and low material cost. $LiNi_{0.5}Mn_{0.5}O_2$ crystallizes in the O3 layered structure (space group $R\bar{3}m$), having typically ~10% interlayer mixing of Ni and Li ions (i.e., ~10% Ni in the Li layer and ~10% Li in the Ni layer[5]), which is much greater than that of $LiCoO_2$ [6] and $LiCo_{1/3}Ni_{1/3}Mn_{1/3}O_2$.[7] Previous studies[8] have shown that decreasing the interlayer mixing can increase the rate capability of $LiNi_{0.5}Mn_{0.5}O_2$, which is attributed to faster Li diffusion with increasing layered character of $LiNi_{0.5}Mn_{0.5}O_2$. More recently, researchers[9,10] have shown that the rate capability of $Li/LiNi_{0.5}Mn_{0.5}O_2$ cells can be improved greatly by applying surface coatings such as AlF_3. Although the physical origin is not understood fully, the coating influence has been attributed to the suppression of transition-metal dissolution and the reduction in the charge-transfer resistance of lithium cells.[9] In this article, we show that annealing of $LiNi_{0.5}Mn_{0.5}O_2$ at 700°C can significantly increase the rate capability of $LiNi_{0.5}Mn_{0.5}O_2$ at room and elevated temperatures. The influence of annealing on the bulk crystal structure and surface chemistry of $LiNi_{0.5}Mn_{0.5}O_2$ quenched from 1000°C is examined by X-ray diffraction (XRD) and X-ray photoelectron spectroscopy (XPS), respectively, which is related to the difference in the rate capability of quenched and annealed $LiNi_{0.5}Mn_{0.5}O_2$.

Experimental

A quenched $LiNi_{0.5}Mn_{0.5}O_2$ sample was prepared by heating a stoichiometric mixture of Li_2CO_3 and $NiMnO_3$ in air at 1000°C for 30 min, which was quenched to room temperature by pressing between two copper plates. An annealed sample was obtained by heating the quenched sample at 700°C in air for 12 h and then cooling slowly to room temperature. The as-prepared quenched and annealed $LiNi_{0.5}Mn_{0.5}O_2$ samples were examined by XRD using a Rigaku diffractometer equipped with a high power rotating copper anode. The Rietveld analysis was conducted using FullProf,[11] where the nominal stoichiometry was constrained and the detailed constraints used were described elsewhere.[12]

The surface chemical compositions of the $LiNi_{0.5}Mn_{0.5}O_2$ samples were investigated by XPS using a Physical Electronics model 5400 spectrometer. The data were collected using nonmonochromatic Mg Kα (1253.6 eV) X-ray source operating at 350 W (15 kV and 23 mA). The analyzed area was set to 1 × 3.5 mm. The C 1s, O 1s, and Li 1s lines were deconvoluted using a Shirley-type background and a combined Gaussian-Lorentzian line shape, whereas the Mn and Ni 2p lines were deconvoluted using an asymmetric line shape. Other analysis details were described elsewhere.[13]

$LiNi_{0.5}Mn_{0.5}O_2$ composite electrodes with 10 wt % poly(vinylidene fluoride) and 10 wt % Super P carbon black were prepared for electrochemical measurements and details can be found in our previous work.[12] A two-electrode cell (Tomcell Co. Ltd., Type TJ-AC), having a lithium metal foil and a $LiNi_{0.5}Mn_{0.5}O_2$ composite electrode separated by two pieces of Celgard 2500, was assembled in an argon-filled glove box (oxygen and water levels less than 2.0 and 1.5 ppm, respectively). 1 M $LiPF_6$ dissolved in ethylene carbonate/dimethyl carbonate (3/7 by volume) (Kishida Chem. Co., Ltd.) was used as the electrolyte. Electrochemical measurements were carried out by using a Solartron 1470 battery testing unit at 30 and 55°C. The rate-capability data for the quenched and annealed samples were collected first from 1/25C (11.2 mA/g or ~0.04 mA/cm^2) and then to 8C (2240 mA/g or ~8.3 mA/cm^2), which were reproduced in multiple cells.

Results and Discussion

Although quenched and annealed $LiNi_{0.5}Mn_{0.5}O_2$ were found to have comparable specific discharge capacities at low rates, annealed $LiNi_{0.5}Mn_{0.5}O_2$ exhibited considerably higher specific capacities than quenched $LiNi_{0.5}Mn_{0.5}O_2$ at rates greater than 1C at 30°C, as shown in Fig. 1. In particular, annealed $LiNi_{0.5}Mn_{0.5}O_2$ was shown to deliver ~120 mAh/g on discharge at 8C, which is much higher than quenched $LiNi_{0.5}Mn_{0.5}O_2$ having ~50 mAh/g at 30°C. Although it is very difficult to compare the rate capability data with those of the previous work in detail due to different C rate definitions, electrode thicknesses, electrode packing densities, etc., the rate capability of quenched $LiNi_{0.5}Mn_{0.5}O_2$ is higher than that of the quenched samples reported previously,[10] whereas the rate capability of annealed $LiNi_{0.5}Mn_{0.5}O_2$ generally compares well with that of state-of-the-art high rate $LiNi_{0.5}Mn_{0.5}O_2$.[8,9,14,15] The rate capability of annealed $LiNi_{0.5}Mn_{0.5}O_2$ was further increased significantly at 55°C, delivering ~180 mAh/g on discharge at 8C. In contrast, there was no significant increase in the rate capability of the quenched sample at 55°C. Moreover, annealed $LiNi_{0.5}Mn_{0.5}O_2$ showed an enhanced capacity retention upon cycling compared to quenched $LiNi_{0.5}Mn_{0.5}O_2$, as shown in Fig. 2. The discharge capacities of annealed $LiNi_{0.5}Mn_{0.5}O_2$ reached a steady-state value of ~190 mAh/g on discharge after 20 cycles to 4.6 V, which is comparable to the highest value reported previously.[2,9,12,15] To understand the origin of the difference in the electrochemical performance characteristics of quenched and annealed $LiNi_{0.5}Mn_{0.5}O_2$, XRD and XPS data are discussed below.

XRD analysis confirmed that both quenched and annealed $LiNi_{0.5}Mn_{0.5}O_2$ had rhombohedral symmetry (space group $R\bar{3}m$), as

* Electrochemical Society Active Member.
z E-mail: shaohorn@mit.edu

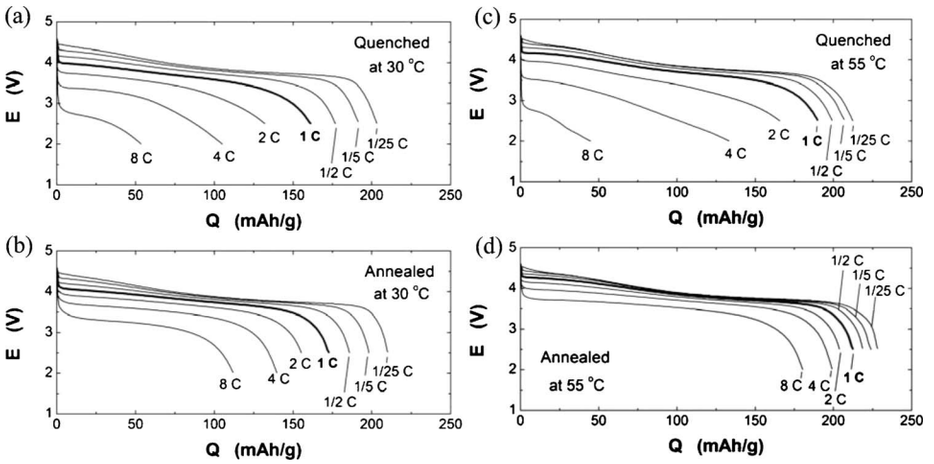

Figure 1. Rate capability of [(a) and (c)] quenched and [(b) and (d)] annealed $LiNi_{0.5}Mn_{0.5}O_2$ in lithium cells discharged at 1/25, 1/5, 1/2, 1, 2, 4, and 8C rates. The cells were discharged at 30 and 55°C. The current density at the 1C rate (based on 280 mA/g) was (a) 1.04, (b) 1.03, (c) 1.04, and (d) 0.77 mA/cm^2. The cells were charged at the 1/5C rate to 4.6 V with holding at 4.6 V for 3 h.

shown in Fig. 3a. The lattice parameters in the hexagonal setting for quenched $LiNi_{0.5}Mn_{0.5}O_2$ [a_{hex} = 2.88982(6) Å and c_{hex} = 14.2960(3) Å] are very comparable to those of annealed $LiNi_{0.5}Mn_{0.5}O_2$ [a_{hex} = 2.88916(6) Å and c_{hex} = 14.2940(3) Å]. In addition, the intensity ratios between the $(003)_{hex}$ and $(104)_{hex}$ peaks are very similar before and after annealing (Fig. 1b), which indicates that there is no significant change in the cation distribution during annealing. This is further confirmed by the Rietveld refinement analysis showing 11 and 9% Ni in the lithium layer per formula unit before and after annealing, which is very comparable to those reported previously for $LiNi_{0.5}Mn_{0.5}O_2$ [8,12,14,16-19] synthesized from solid-state routes. The minor differences in the structural parameters of quenched and annealed $LiNi_{0.5}Mn_{0.5}O_2$ are very unlikely to give rise to the apparent different rate capability measured in this study.

The XPS analysis of the C 1s and O 1s regions indicated that the amount of surface carbonate species for annealed $LiNi_{0.5}Mn_{0.5}O_2$ was significantly lower than that of quenched $LiNi_{0.5}Mn_{0.5}O_2$, as shown in Fig. 4. The C 1s line was deconvoluted into four components: (*i*) adventitious hydrocarbon at 285.0 eV; (*ii*) carbon in C—O (286.5 eV) and (O—C—O/C═O) (~288/287.5 eV [20]); (*iii*) carbon in the carboxylic groups (O—C═O) at 289 eV; and (*iv*) carbon in the carbonate (CO_3^{2-}) form (near 290.6 eV). Of significance, the surface carbonate contribution to C 1s for quenched $LiNi_{0.5}Mn_{0.5}O_2$ is considerably larger than that for annealed $LiNi_{0.5}Mn_{0.5}O_2$, as shown in Table I. Correspondingly, in the O 1s region, the relative intensity of surface oxygen species such as surface terminated oxy-

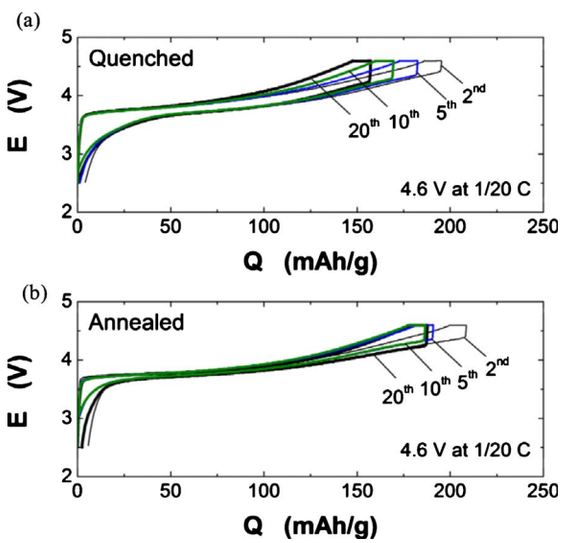

Figure 2. (Color online) Cycling performance of (a) quenched $LiNi_{0.5}Mn_{0.5}O_2$ and (b) annealed $LiNi_{0.5}Mn_{0.5}O_2$ between 2.5 and 4.6 V at a rate of 1/20C and then held at 4.6 V for 3 h.

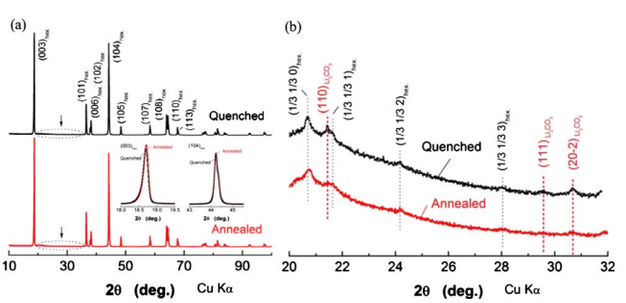

Figure 3. (Color online) (a) XRD patterns of quenched and annealed $LiNi_{0.5}Mn_{0.5}O_2$. The highlighted $(003)_{hex}$ and $(104)_{hex}$. Bragg peaks are shown for comparison. The trace of the impurity phase has been confirmed for the quenched sample as shown in (b).

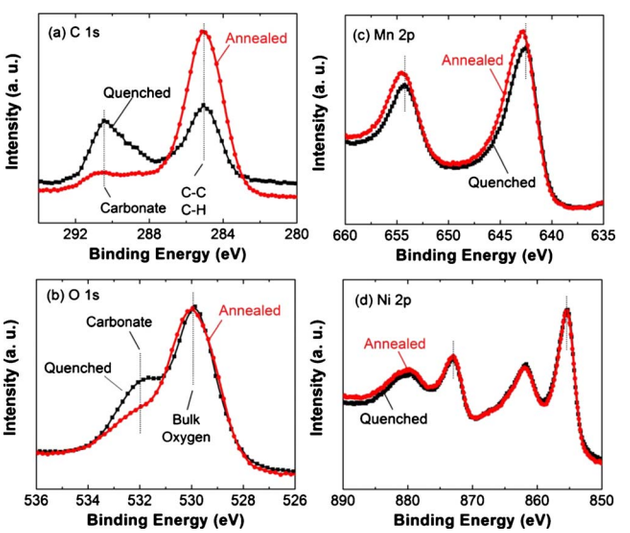

Figure 4. (Color online) X-ray photoelectron spectra of (a) C 1s, (b) O 1s, (c) Mn 2p, and (d) Ni 2p photoemission lines for quenched and annealed $LiNi_{0.5}Mn_{0.5}O_2$. The C 1s intensity of the quenched sample was magnified 1.5 times for better comparison, whereas other data are shown as measured.

Table I. Summary of XPS results including BE in eV, fwhm, and atomic percents.

		Quenched			Annealed		
Peak	Assignment	BE (eV)	fwhm (eV)	Atom %	BE (ev)	fwhm (eV)	Atom %
C ls	Hydrocarbon (285.0 eV)	285.0	2.25	5.0	285.0	2.35	14.6
	C—O (~286.1 eV)/O—C—O/C═O (~287 eV)	287.0	1.6	0.8	287.3	1.34	0.4
	O—C═O(~289 eV)	288.7	1.67	1.3	288.7	2.00	1.2
	CO_3(~290.3 eV)	290.4	1.88	3.1	290.7	2.00	1.3
Total C				10.2			17.5
O ls	Lattice oxygen in $LiNi_{0.5}Mn_{0.5}O_2$(~529.8 eV)	529.8	1.83	40.9	529.9	2.14	43.0
	Surface oxygen in $LiNi_{0.5}Mn_{0.5}O_2$(~531.7 eV) and carbonates CO_3 (~532.1 eV)	532.0	2.11	18.8	532.3	2.27	10.6
Total O				59.7			53.6
Mn 2p3/2	$LiNi_{0.5}Mn^{4+}_{0.5}O_2$(~642.5 eV)	642.4	2.69	12.5	642.7	2.74	12.8
Ni 2p3/2	$LiNi^{2+}_{0.5}Mn_{0.5}O_2$(854.2–854.9 eV) $LiNi^{3+}_{0.5}Mn_{0.5}O_2$(855.2–855.5 eV)	855.2	2.35	10.5	855.3	2.31	10.3
Ni 2p3/2 sat.		861.7	3.87	7.2	861.8	3.66	5.8
	Ni/Mn		1.42			1.26	

fwhm is full width at half-maximum.

gen atoms[21] and oxygen atoms doubly bound to carbon atoms in Li_2CO_3 (~532.0 eV [22]) to lattice oxygen (529.9 eV) is greater for quenched than annealed $LiNi_{0.5}Mn_{0.5}O_2$. This result agrees well with the observation that a small amount of Li_2CO_3 was detected in the XRD data of quenched but not of annealed $LiNi_{0.5}Mn_{0.5}O_2$, as shown in Fig. 3b.

The XPS analysis of the Mn 2p3/2 region showed that Mn was present as a mixture of Mn^{3+} and Mn^{4+} for quenched $LiNi_{0.5}Mn_{0.5}O_2$ and mostly as Mn^{4+} for annealed $LiNi_{0.5}Mn_{0.5}O_2$. The Mn 2p3/2 binding energy (BE) for quenched $LiNi_{0.5}Mn_{0.5}O_2$ (642.4 eV) fell between the values of Mn_2O_3 (642.2 eV) and MnO_2 (642.8 eV) compounds measured in this study and reported previously,[23] whereas that of annealed $LiNi_{0.5}Mn_{0.5}O_2$ (642.7 eV) is very close to that of MnO_2. However, as the Ni 2p3/2 BE values for quenched (855.2 eV) and annealed (855.3 eV) $LiNi_{0.5}Mn_{0.5}O_2$ are close to those reported for NiO (855.0 eV) [24] after adjusting the spectrometer calibration to our scale and the weighted average of its double peak structure (855.4 eV) [25] and much lower than that of $LiNiO_2$ (856.0 eV),[26] it is concluded that surface Ni is present as Ni^{2+}. In addition, the atomic Ni/Mn ratio of quenched (1.42) is higher than that of annealed (1.26) $LiNi_{0.5}Mn_{0.5}O_2$, both of which are higher than the nominal value of 1, as shown in Table I. The Ni enrichment on the surface can be a result of the partial surface decomposition of layered $LiNi_{0.5}Mn_{0.5}O_2$ at 1000°C to form impurity Li_2O- and NiO-like phases on the surface (one limiting case can be $LiNi_{0.5}Mn_{0.5}O_2 \rightarrow 0.5Li_2O + 0.25NiO + 0.25NiMn_2O_4 + 0.125O_2$, which yields only Mn^{3+}),[27] where Li_2O can react with CO_2 upon cooling to produce lithium carbonate, which was detected by XRD and XPS analyses. The major phase on the surface would be Mn-enriched and Ni-deficient (relative to nominal $LiNi_{0.5}Mn_{0.5}O_2$), and having Mn/Ni ratios greater than 1 and mixed valence states of Mn^{3+} and Mn^{4+}.[4] Such a process might be reversed upon subsequent annealing.

The increased rate capability of annealed $LiNi_{0.5}Mn_{0.5}O_2$ can be attributed in part to the reduction of lithium carbonate on the surfaces of quenched $LiNi_{0.5}Mn_{0.5}O_2$ particles by annealing, which can decrease the resistance to electron and charge transfer of lithium intercalation and deintercalation. This is further supported by XPS findings that the cycled quenched $LiNi_{0.5}Mn_{0.5}O_2$ electrode after 20 cycles have more surface carbonate species than the similarly cycled annealed $LiNi_{0.5}Mn_{0.5}O_2$ (not shown). In addition, it is hypothesized that annealed $LiNi_{0.5}Mn_{0.5}O_2$ with a particle surface stoichiometry closer to $LiNi^{2+}_{0.5}Mn^{4+}_{0.5}O_2$ would have less Mn dissolution (dissolution of soluble Mn^{2+} ions via a disproportionation reaction from $Mn^{3+}_{solid} \rightarrow Mn^{2+}_{solution}$ and Mn^{4+}_{solid}),[28] and thus contribute a smaller impedance increase in lithium cells than quenched $LiNi_{0.5}Mn_{0.5}O_2$ having more surface Mn^{3+}, which can render higher rate capability for annealed $LiNi_{0.5}Mn_{0.5}O_2$. This hypothesis agrees with the fact that the difference in the rate capability of quenched and annealed $LiNi_{0.5}Mn_{0.5}O_2$ is greater at 55°C than at room temperature as the Mn dissolution[29] and growth of impeding films are expected to increase at higher testing temperatures.

Conclusions

We showed that an additional annealing step can significantly enhance the rate capability of $LiNi_{0.5}Mn_{0.5}O_2$ relative to quenched $LiNi_{0.5}Mn_{0.5}O_2$. The enhanced rate capability can be attributed to making surface chemistry more stoichiometric having $LiNi^{2+}_{0.5}Mn^{4+}_{0.5}O_2$ during annealing by reducing surface Li_2CO_3- and Mn^{3+}-containing phases.

Acknowledgments

This work was supported by the Assistant Secretary for Energy Efficiency and Renewable Energy, Office of FreedomCAR and Vehicle Technologies of the DOE (DE-AC03-76SF00098 with LBNL).

Massachusetts Institute of Technology assisted in meeting the publication costs of this article.

References

1. T. Ohzuku and Y. Makimura, *Chem. Lett.*, **30**, 744 (2001).
2. Z. H. Lu, D. D. MacNeil, and J. R. Dahn, *Electrochem. Solid-State Lett.*, **4**, A191 (2001).
3. Y. Koyama, Y. Makimura, I. Tanaka, H. Adachi, and T. Ohzuku, *J. Electrochem. Soc.*, **151**, A1499 (2004).
4. J. Reed and G. Ceder, *Electrochem. Solid-State Lett.*, **5**, A145 (2002).
5. H. Kobayashi, Y. Arachi, H. Kageyama, and K. Tatsumi, *J. Mater. Chem.*, **14**, 40 (2004).
6. S. Levasseur, M. Menetrier, E. Suard, and C. Delmas, *Solid State Ionics*, **128**, 11 (2000).
7. N. Yabuuchi, Y. Koyama, N. Nakayama, and T. Ohzuku, *J. Electrochem. Soc.*, **152**, A1434 (2005).
8. K. S. Kang, Y. S. Meng, J. Breger, C. P. Grey, and G. Ceder, *Science*, **311**, 977 (2006).
9. Y. K. Sun, S. T. Myung, B. C. Park, and H. Yashiro, *J. Electrochem. Soc.*, **155**, A705 (2008).
10. H. C. Lin, J. M. Zheng, and Y. Yang, *Mater. Chem. Phys.*, **119**, 519 (2010).
11. J. Rodríguez-Carvajal, *J. Phys. B*, **192**, 55 (1993).
12. N. Yabuuchi, S. Kumar, H. H. Li, Y. T. Kim, and Y. Shao-Horn, *J. Electrochem. Soc.*, **154**, A566 (2007).
13. Y. C. Lu, A. N. Mansour, N. Yabuuchi, and Y. Shao-Horn, *Chem. Mater.*, **21**, 4408 (2009).
14. K. S. Lee, S. T. Myung, J. S. Moon, and Y. K. Sun, *Electrochim. Acta*, **53**, 6033 (2008).
15. Y. Makimura and T. Ohzuku, *J. Power Sources*, **119–121**, 156 (2003).
16. Y. Arachi, H. Kobayashi, S. Emura, Y. Nakata, M. Tanaka, T. Asai, H. Sakaebe, K.

Tatsumi, and H. Kageyama, *Solid State Ionics*, **176**, 895 (2005).
17. Z. H. Lu, L. Y. Beaulieu, R. A. Donaberger, C. L. Thomas, and J. R. Dahn, *J. Electrochem. Soc.*, **149**, A778 (2002).
18. N. Yabuuchi, Y. T. Kim, H. H. Li, and Y. Shao-Horn, *Chem. Mater.*, **20**, 4936 (2008).
19. J. Bréger, Y. S. Meng, Y. Hinuma, S. Kumar, K. Kang, Y. Shao-Horn, G. Ceder, and C. P. Grey, *Chem. Mater.*, **18**, 4768 (2006).
20. H. Ago, T. Kugler, F. Cacialli, W. R. Salaneck, M. S. P. Shaffer, A. H. Windle, and R. H. Friend, *J. Phys. Chem. B*, **103**, 8116 (1999).
21. J. C. Dupin, D. Gonbeau, H. Benqlilou-Moudden, P. Vinatier, and A. Levasseur, *Thin Solid Films*, **384**, 23 (2001).
22. S. Verdier, L. El Ouatani, R. Dedryvere, F. Bonhomme, P. Biensan, and D. Gonbeau, *J. Electrochem. Soc.*, **154**, A1088 (2007).
23. N. Treuil, C. Labrugere, M. Menetrier, J. Portier, G. Campet, A. Deshayes, J. C. Frison, S. J. Hwang, S. W. Song, and J. H. Choy, *J. Phys. Chem. B*, **103**, 2100 (1999).
24. L. J. Matienzo, L. I. Yin, S. O. Grim, and W. E. Swartz, *Inorg. Chem.*, **12**, 2762 (1973).
25. A. N. Mansour, *Surf. Sci. Spectra*, **3**, 231 (1994).
26. A. N. Mansour, *Surf. Sci. Spectra*, **3**, 279 (1994).
27. C. Barriga, J. M. Fernandez, M. A. Ulibarri, F. M. Labajos, and V. Rives, *J. Solid State Chem.*, **124**, 205 (1996).
28. M. M. Thackeray, Y. Shao-Horn, A. J. Kahaian, K. D. Kepler, J. T. Vaughey, and S. A. Hackney, *Electrochem. Solid-State Lett.*, **1**, 7 (1998).
29. A. Blyr, C. Sigala, G. Amatucci, D. Guyomard, Y. Chabre, and J. M. Tarascon, *J. Electrochem. Soc.*, **145**, 194 (1998).